A novel sp3 Carbon Allotrope with 4+5+6+7+8 odd-even ring

Tao Yu[1], Sheng-Cai Zhu[1*], Yanglong Hou[1*]

1. School of Materials, Shenzhen Campus of Sun Yat-sen University, Shenzhen 518107, China.

Corresponding Author

* e-mail: S.-C.Z. (zhushc@mail.sysu.edu.cn), Y.-L.H (hou@mail.sysu.edu.cn)

The XRD standard cards of Y carbon under different pressures are presented in **Figure S1**.

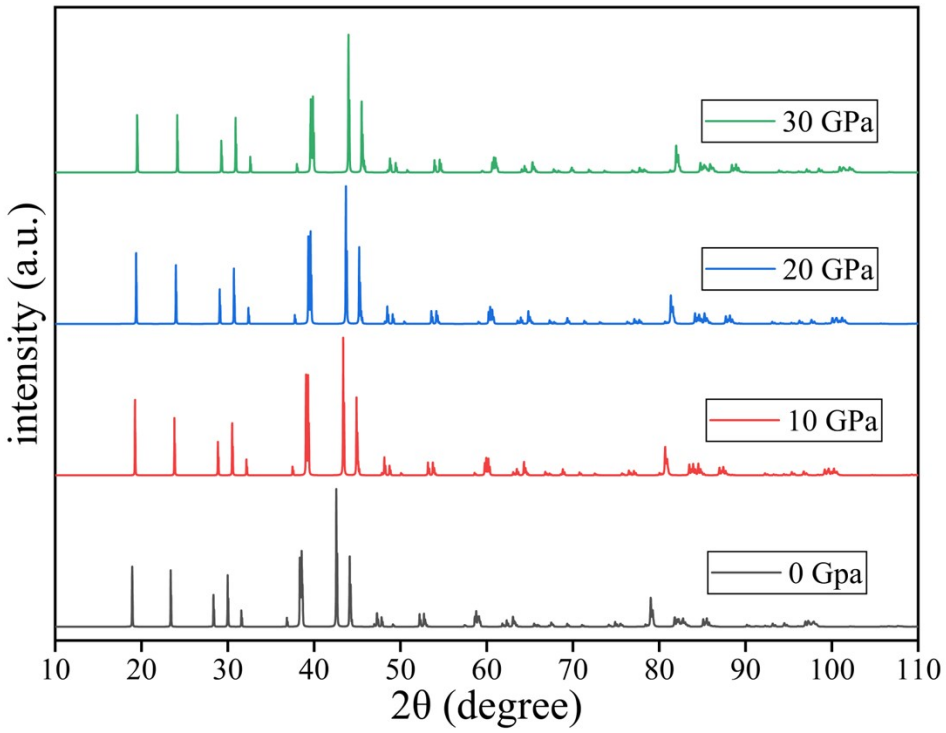

Figure S1. XRD patterns of Y carbon under different pressures.

SSW method visits PES with a small step-size by exploiting the second-derivative (vibrational mode) information. SSW is able to sample the structural patterns at the transition region, and this allow finding unknown chemical reactions. The SSW method combines bias-potential-driven dynamics and the Metropolis Monte Carlo (MC) method. The former is a standard technique utilized to overcome high barriers between minima on a PES, and the latter is a common method in PES sampling to select states according to the Boltzmann distribution, The SSW method adopts a random mode generation and a constrained softening technique to obtain an optimal mode along which the bias-potentials are added. Combine with these two methods, SSW can overcome the high barriers on PES and identifies both minima and the low energy pathways between them. Since we are only using this soft, it is not discussed in our manuscript. If you want to learn more about how SSW works, please refer to the literature by Liu, et al., (Acc. Chem. Res.2020, 53, 10, 2119).

NN potential utilize the basic principles of high dimensional neural network (HDNN) and the local chemical environment adopt the power-type structural descriptor (PTSD), with those basic principles, we can make sure that the supercell of the structure (the increase of atom numbers) do not change the energy per atom and the input of the ML model is continuous and derivable with respect to the atomic coordinate. The training process of NN potential is shown in Figure S2. Table S1 is the training dataset of NN potential we used. Figure S3 is the energy diagram of graphite, CD and HD calculated by NN and DFT respectively under different pressures, which shows the high accuracy of NN potential.

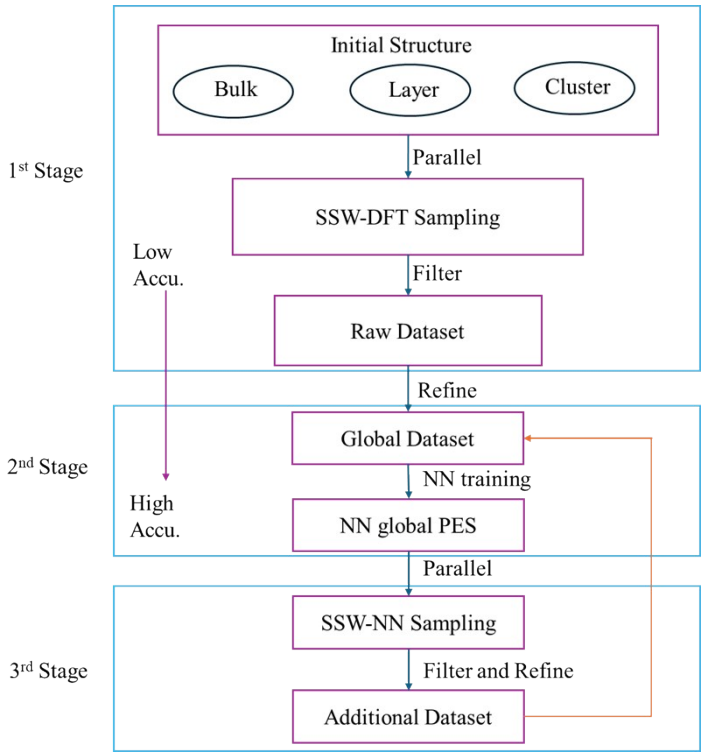

Figure S2. NN potential training process.

Table S1. Components of NN training dataset.

Species	Atom number	Cluster	Layer	Bulk	Total
C6	6	1299	9	2821	4129
C8	8	0	37	833	870
C9	9	0	0	85	85
C12	12	0	16	3245	3261
C14	14	0	1	133	134
C16	16	0	3400	28192	31592
C18	18	0	0	62	62
C24	24	0	9	581	590
C28	28	0	0	69	69
C30	30	0	11	345	356
C31	31	0	629	504	1133
C32	32	0	1186	14574	15760
C36	36	0	4	261	265
C48	48	0	13	446	459

C56	56	0	5	76	81
C57	57	0	0	38	38
C58	58	0	0	35	35
C59	59	0	83	2	85
C60	60	0	0	88	88
C61	61	0	95	41	136
C62	62	0	172	178	350
C64	64	0	187	1761	1948
C128	128	0	0	493	493
Total	\	1299	5857	54863	62019

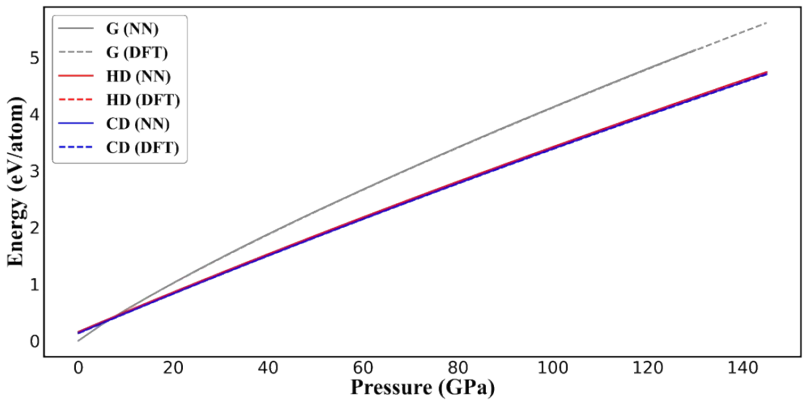

Figure S3. Comparison of E-P plot by DFT and NN calculation. G: graphite, CD: cubic diamond, HD: hexagonal diamond. The plot scarcely distinguishes DFT and NN data, indicating the high accuracy of NN.

We calculated the ELF of Y in Figure S4, it's obvious that the valence electrons are in a localization state, and all atoms can form covalent bonds with adjacent atoms.

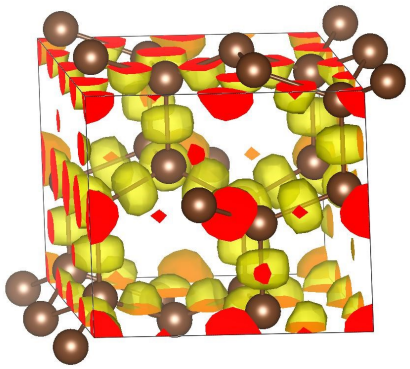

Figure S4. ELF diagram of Y. The ELF isosurface is 0.75.

To test the mechanical property of Y carbon, we calculate the mechanical properties of Y carbon and CD with VASP, the value of NFREE was identified as 4 to work out a more accurate rigid matrix which the results are shown in **Table S2**, VASPKIT[1] was used to process the rigid matrix and obtain its three-dimensional mechanical diagram, as shown in **Figure S5** and **Figure S6**. From Young's modulus, it can be seen that Y carbon is difficult to deform in the [001] and [010] directions while CD is in the [111] orientation. From the bulk modulus, CD is isotropic in compressibility while Ycarbon is difficult to compress (greater than CD) in the [001] orientation. It can be seen from the shear modulus that CD shows easy slip at (110) [111], which is consistent with the experiment, while CD shows easy slip at (001) [010] and (001) [100], which provides guidance for the subsequent molecular dynamics. It's obvious that Y carbon has a bulk modulus of up to 407 GPa, a shear modulus of 894 GPa, and a Young's modulus of 372 GPa. Simultaneously, CD has a bulk modulus of up to 442 GPa, a shear modulus of 1032 GPa, and a Young's modulus of 465 GPa. Y carbon has approximately 90% mechanical properties of CD.

Table S2. The rigid matrix of Y carbon and CD at 0 GPa.

Rigid matrix (CD)					
1061	132	132	0	0	0
132	1061	132	0	0	0
132	132	1061	0	0	0
0	0	0	569	0	0
0	0	0	0	569	0
0	0	0	0	0	569
Rigid matrix (Y carbon)					
1017	75	156	0	-4	0
75	1153	45	0	-1	0
156	45	1159	0	-17	0
0	0	0	447	0	-2
-4	-1	-17	0	462	0
0	0	0	-2	0	372

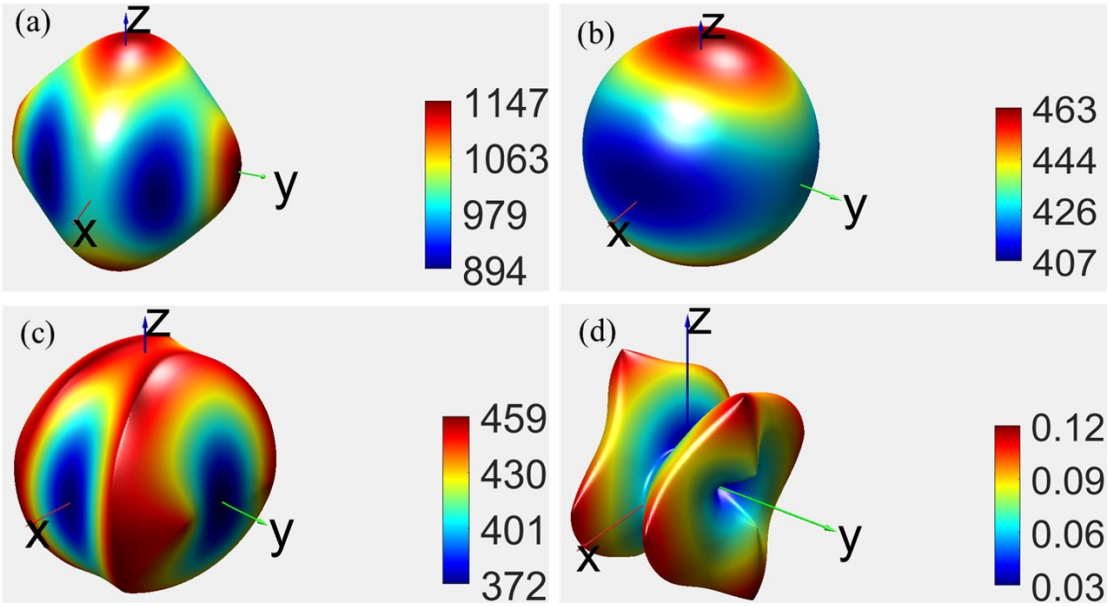

Figure S5. Mechanical properties of Y carbon. (a) Youngs modulus. (b)Bulk modulus. (c)Shear modulus. (d) Poisson ratio.

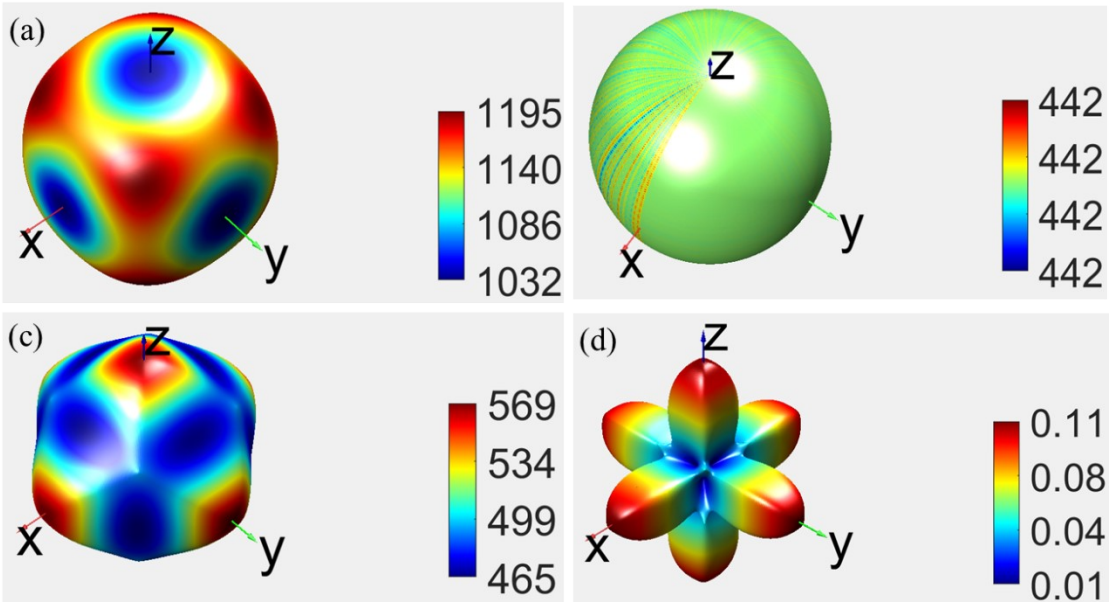

Figure S6. Mechanical properties of CD. (a) Youngs modulus. (b) Bulk modulus. (c)Shear modulus. (d) Poisson ratio

In addition, we use molecular dynamics to further explore the hardness of Y carbon, we compared two classical shear methods in LAMMPS which is deform and velocity. Velocity is a process of simulating pure shear, while deform method resemble to test shear hardness. CD was used as the benchmark, we found that the hardness obtained by deform method is in line with the experimental expectation, hence, deform method is used for the hardness simulation in this paper.

To find the most easily yielding plane and orientation of Y carbon. A supercell with more than 400 atoms was constructed, and after energy minimization and thermodynamic relaxation, we conducted shear tests on its different planes and orientations which reached 100% strain within 0.1ns and showed their stress-strain curves in **Figure S7**. By comparing their ultimate strength, we found its slip plane and slip orientation, i.e. (001) $[0\bar{1}0]$ with a shear hardness of 81.9 GPa. For comparison, we simulated the different planes and orientations of the CD, and the results are shown in **Figure S8**, which we can see its slip plane and slip orientation, i.e. (111) $[\bar{1}10]$ with a shear hardness of 87 GPa.

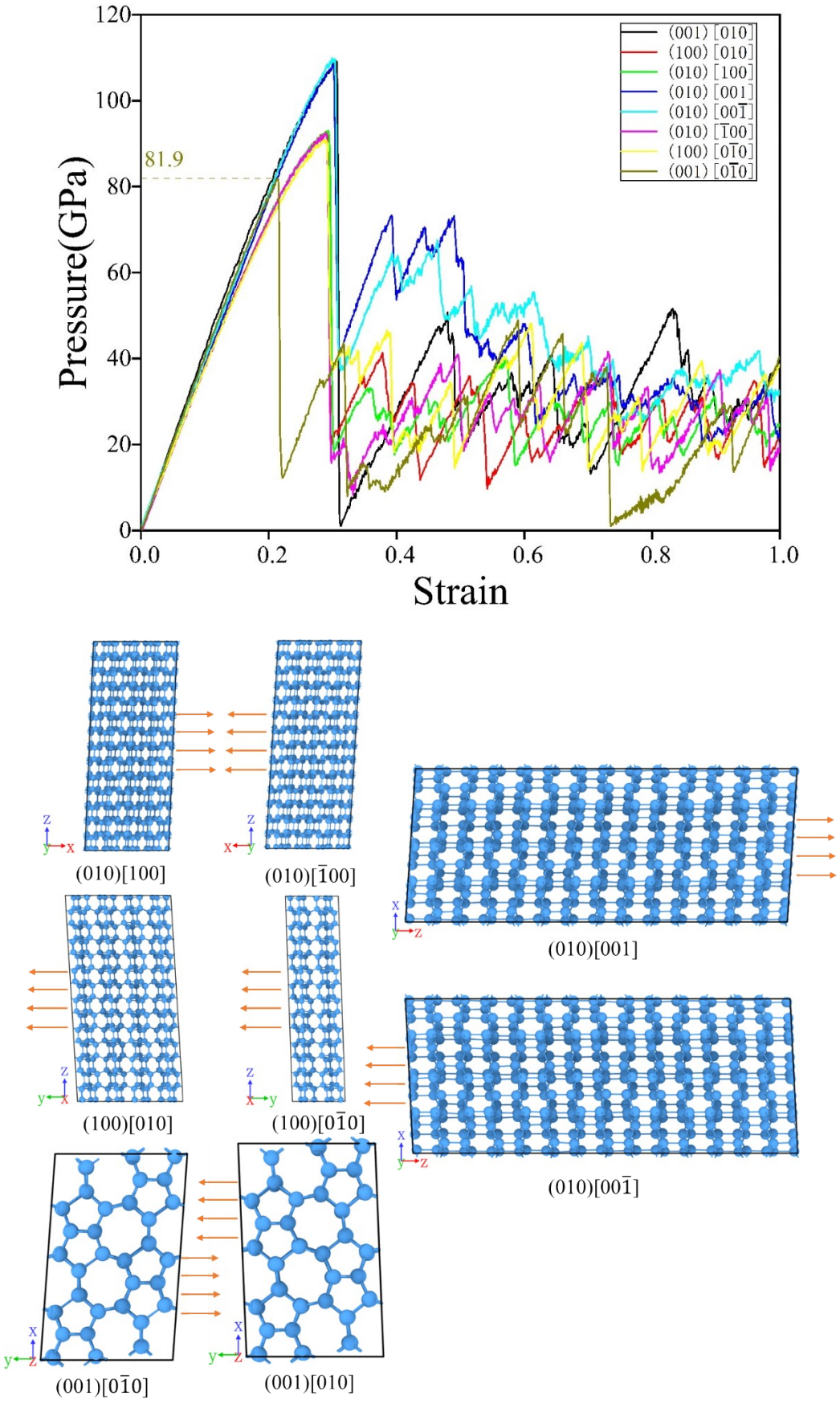

Figure S7. Stress-strain curves and structure diagram of Y carbon shearing in different orientations.

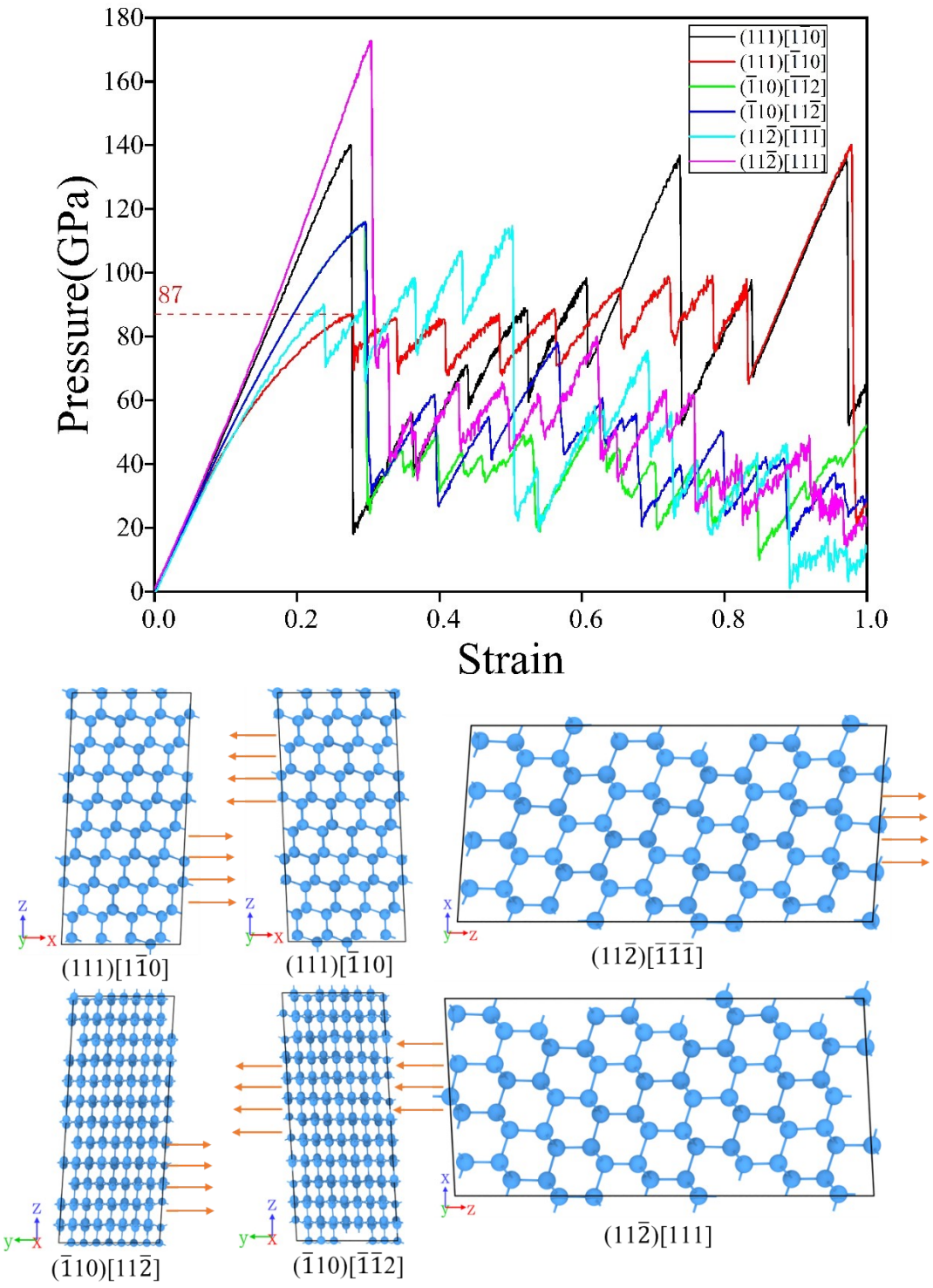

Figure S8. Stress-strain curves and structure diagram of CD shearing in different orientations.

After we built the two interfaces, we used LSAP for structural optimization with 200 SSW steps, more than 70 local minima were obtained, among which 5 were optimal structure. After screening, we obtained the final optimized structure which as show in **Figure S9**. We count the atoms of Y carbon and HD that make up the two kinds of interfaces, and had the average energy of C atoms calculated, respectively, the lattice constants of the surface before optimization and the interface after optimization are recorded, all the information is given in **Table S3**. We use the formula (1) and (2) to calculate the interface energy(γ) and strain(ΔS). For the interface of Y carbon (100) and HD (001), the total Energy of final structure is -1363.498 eV. We calculated that γ=0.058 eV/Å², ΔS = 2%. For Y carbon (001) and HD (001), the total Energy of final structure is -1553.183 eV. So the γ=0.580 eV/Å², ΔS=3.7%.

$$\gamma = \frac{E_{Total} - E_{Ycarbon} - E_{HD}}{2S_{Final}} \#(1)$$

$$\Delta S = \frac{S_{Final} - S_{HD}}{S_{Final}} \#(2)$$

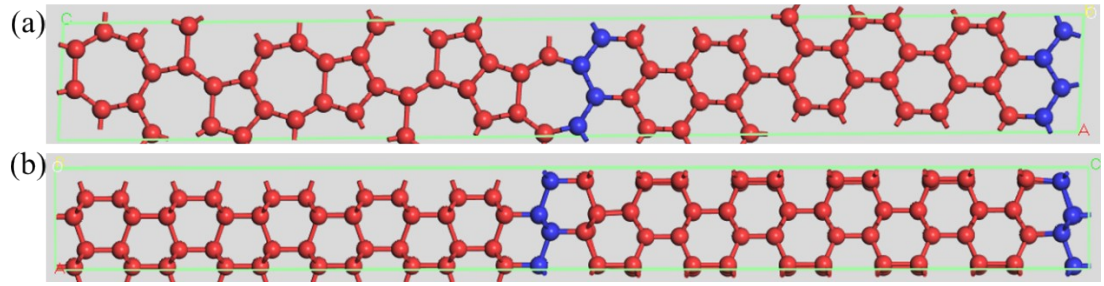

Figure S9. Two kinds of interface after optimization. (a) $(001)_Y//(100)_{HD}$, $[100]_Y//[010]_{HD}$. (b) $(001)_Y//(001)_{HD}$, $[010]_Y//[001]_{HD}$.

Table S3. The parameter changes of two kinds of interface structure after optimization.

Y carbon (100)- HD (001)				
	atoms	Energy/atom (eV)	U (Å)	V (Å)
Ycarbon	72	-8.894	4.832	4.244/
HD	80	-9.069	4.337	5.016
Final Surface			4.951	4.227
Y carbon (001) - HD (001)				
	atoms	Energy/atom (eV)	U (Å)	V (Å)
Ycarbon	96	-8.894	4.825	4.832

HD	80	-9.069	4.337	5.016
Final Surface			4.543	4.972

Structure of Y carbon at 0 GPa.

PBC	4.82511829	4.83204292	4.24365406	89.99980485	89.99976304	76.14564307		
C	0.454885179	0.547245285	0.274524607	CORE	1 C	C	0.0000	1
C	5.527271114	4.144276625	2.396336093	CORE	2 C	C	0.0000	2
C	5.527278390	4.144259469	3.969122252	CORE	3 C	C	0.0000	3
C	0.454890597	0.547224051	1.847311843	CORE	4 C	C	0.0000	4
C	1.131087372	2.786079739	0.265353792	CORE	5 C	C	0.0000	5
C	4.851083809	1.905439602	2.387263844	CORE	6 C	C	0.0000	6
C	4.851071975	1.905423455	3.978288403	CORE	7 C	C	0.0000	7
C	1.131076545	2.786060831	1.856379077	CORE	8 C	C	0.0000	8
C	3.633026073	2.592047929	0.290329849	CORE	9 C	C	0.0000	9
C	2.349121976	2.099451672	2.412080464	CORE	10 C	C	0.0000	10
C	2.349136717	2.099459546	3.953308370	CORE	11 C	C	0.0000	11
C	3.633038430	2.592047827	1.831557178	CORE	12 C	C	0.0000	12
C	4.045357480	4.167138659	0.284455910	CORE	13 C	C	0.0000	13
C	1.936804804	0.524356287	2.406251246	CORE	14 C	C	0.0000	14
C	1.936804186	0.524365753	3.959191076	CORE	15 C	C	0.0000	15
C	4.045356642	4.167143069	1.837395466	CORE	16 C	C	0.0000	16

References

1 V. Wang, N. Xu, J.-C. Liu, G. Tang, and W.-T. Geng, VASPKIT: A user-friendly interface facilitating high-throughput computing and analysis using VASP code, *Comput. Phys. Commun.*, 2021, **267**, 108033.